HDPE Surface Functionalization by Low-Energy Ion-Beam Irradiation under a Reactive O_2 Environment and Its Effect on the HDPE/Nylon 66 Blend

Hyong-Jun Kim,[†,‡] Ki-Jun Lee,[‡] Yongsok Seo,[*,†] Soonjong Kwak,[†] and Seok-Keun Koh[§]

Polymer Processing Laboratory, Korea Institute of Science and Technology, P.O. Box 131, Cheongryang, Seoul, Korea 130-650; Department of Chemical Engineering, Seoul National University, Shinlimdong 56-1, Kwanak-ku, Seoul, Korea; Thin Film Technology Center, Korea Institute of Science and Technology, P.O. Box 131, Cheongryang, Seoul, Korea 130-650

Received August 4, 2000; Revised Manuscript Received December 8, 2000

ABSTRACT: A low energy Ar^+ ion-beam was used to modify the surface of a high-density polyethylene (HDPE) dry powder. The modification reaction was promoted by the oxygen gas injected during the irradiation. This simple modification route is characterized as a heterogeneous, solvent-free, environmentally favorable process. The surface functional groups of the modified HDPE were confirmed with X-ray photoelectron spectroscopy and Fourier transform infrared spectroscopy as being various oxygen-containing functional groups. The concentration of the functional groups varied rapidly with the irradiation time, reached a maximum value and then slowly decreased. Because of the low-energy characteristics of the ion beam, the changes in the molecular weight, the melting temperature, and the crystallinity of the modified HDPE were not significant, as evidenced by gel-permeation chromatography and differential scanning calorimetry. The rheological behavior of an HDPE/nylon 66 (Ny66) blend, which depends on the blend composition, was complicated due to immiscibility whereas the ion-beam-irradiated HDPE/Ny66 blend showed a more systematic behavior. Also, the compatibility effect of ion-beam-treated HDPE was investigated in the blend of HDPE/ Ny66. In the ion-beam-irradiated HDPE/blends, a significant decrease in the domain size of the dispersed phase was observed. Theoretical models were used to estimate the interfacial tension of HDPE/Ny66 blends. The calculated interfacial tension of an ion-beam-treated HDPE/Ny66 blend was less than that of a nontreated HDPE/Ny66 blend, indicating a greater interaction between the ion-beam-treated HDPE and the Ny66 phases. In addition, the mechanical properties of the ion-beam-treated HDPE/Ny66 blend showed a positive deviation from the rule of mixture. Finally, an explanation of the compatibilizing effect of ion-beam-treated HDPE is presented.

Introduction

Mixing two or more polymers together to form polymer blends or alloys is a well-established method to achieve a specified portfolio of physical properties without the need to synthesize specialized polymer systems.[1,2] Compatibilization, the modification of normally immiscible blends to give alloys with improved end-use performance, is an important factor in almost all commercial blends and has been the subject of numerous experimental investigations, many of which remain proprietary.[3,4] The most prevalent methods of achieving compatibility are addition of a compatibilizer (block or graft copolymers), in situ grafting and/or polymerization by reactive blending (functional/reactive polymers).[5] Reactive blending is different from other compatibilization routes in that the blend components themselves are either chosen or modified so that the reaction occurs during melt blending, with no need for the addition of a separate compatibilizer.[6] This route has many commercial applications, for example, in blends of polycarbonates and polyesters and in toughened polyamides.[5,6] A number of reactive blending mechanisms may be exploited. One is the formation of an in situ graft or a block copolymer by chemical reactions between reactive groups on component polymers.[7] Another is the attachment of a functional group, which can interact with other polymers, on the polymer backbone. In summary, many different methods have been investigated for functionalizing polymers.[1,3,5]

Modification of polymers has become an important research area in the plastics industry. Especially, the modification of chemically inert polymers such as polyolefins has attracted much attention because the absence of any functional groups has limited their use in many applications where adhesion, compatibility, printability, or hydrophilicity are required. Various modification methods have been employed, including wet chemical methods and vacuum techniques. In the conventional wet chemistry approach, an active species is transported to a polymer surface immersed in a solvent. Usually the process requires a number of steps in order to achieve the desired surface functionality. Vacuum technologies, on the other hand, involve the exposure of a polymer surface to a plasma, a photon source, an electron beam or an ion beam.[8,9] The plasma or gas phase approach promises to be more efficient, and requires no solvent and fewer chemicals. The irradiation methods have their own merit; i.e., chemical or physical changes occur on the polymer surface without affecting the bulk properties. Among the irradiation methods, polymer surface modification by ion-beam irradiation was intensively investigated in the 1990s.[10,11] However, its application to polymers was limited due to undesirable side reactions such as polymer degradation and cross-linking.[11] Recently, we developed a novel process, low-energy ion-beam irradiation under a reactive gas environment, for polymer surface modification.[12,13] Most other vacuum

* To whom correspondence should be addressed. E-mail: ysseo@kist.re.kr.
† Polymer Processing Laboratory, KIST.
‡ Seoul National University.
§ Thin Film Technology Center, KIST.

10.1021/ma0013760 CCC: $20.00
Published on Web 03/17/2001

methods have adopted high-energy ion-beam irradiation,[11] but our method employs a low-energy ion-beam (less than 5 keV) that is strong enough to activate the polymer surface and additional gas molecules.[14] This low-energy ion-beam irradiation reduces chain degradation or the cross-linking of irradiated polymers, and added gas molecules, such as oxygen or ammonia, are then chemically adsorbed onto the surface to form functional groups.[15] These functional groups can then react or interact with other functional groups in other polymers. The beam conditions, such as the energy, the density and the dose, can be varied over wide ranges in precisely controllable ways, allowing good reproducibility.[12−15] Usually, these treatments have been used to modify the surfaces of films or fibers, to promote printability, or in multiplayer systems to improve the adhesion between the substrate and the polymers.[12−15] Surprisingly, little effort has been expended to extend these treatments to the area of polymer blends. Since polymer surface modification, hence functionalization, can change the interactions between different polymer molecules in blends, it can pave the way for improving the physical properties of immiscible polymer blends.[16]

As an ab initio study, we investigated the feasibility of using ion-beam modification to decide the class of the functional groups and the rate of functional group incorporation. In this study, high-density polyethylene (HDPE) in dry powder form was modified by using Ar^+ ion-beam irradiation with a flowing O_2 environment in a specially designed reactor. The chemical and physical properties of the modified polymers and the effect of HDPE modification on the physical properties of the HDPE/nylon 66 (Ny66) blend are reported. Using the correlation between the rheology and the morphology of the blends, we also investigated the change in the interfacial property with surface functionalization.

Experimental Section

Materials. The materials employed in this study were commercial polyamide (nylon 66 (Ny66)) and high-density polyethylene (HDPE). The HDPE was supplied by Taehan Yuhwa Chemicals (Korea). The weight-average molecular weight, M_w, was 1.8×10^5, and the polydispersity index was 11.95. The HDPE was supplied in powder form, and the powder passed through a mesh of 100 mesh size was used. The Ny 66 was a DuPont product (Zytel E101). Argon and oxygen gases of 99.99% purity were used. Formic acid (Junsei Chemical Co.) was used as received.

Ion-Beam Irradiation. The ion-beam-assisted reaction system was composed of a conventional ion-beam system, a reactive gas feeding system, and the polymer−sample (powder or pellet) mixing bowl. Figure 1 shows a schematic diagram of the ion-beam irradiation reactor. The working pressure in the reaction chamber was kept under 10^{-4} Torr. The Ar^+ ion beam was generated from a 5 cm cold-hollow cathode ion-source, and its potential energy was maintained at less than 1 keV. The currents of the ions were controlled by the discharge voltage and the ion-beam potential. The discharge current was 0.4 A, and the ion fluence was varied between 1.6×10^{18} to 1.3×10^{20} ions/cm^2. The ion fluence was measured by using a Faraday cup placed slightly above the polymer powder. The flow rate of Ar gas, which was ionized to Ar^+ by the ion source, was fixed at 2 sccm. The mixing bowl was equipped with a rotor blade for uniform mixing during ion-beam irradiation. Reactive O_2 gas was constantly injected from the bottom of the chamber. The flow rate of the O_2 gas was 3 sccm, and was controlled by using a mass flow controller (MassFlo 9121).

The Ny66 pellets and the HDPE powder were dried in a vacuum oven at 100 °C for 24 h. The dried HDPE powder (100 g) was put into the mixing bowl in the ion-beam chamber, and a vacuum under 10^{-4} Torr was applied. The mixing bowl was covered with a circular Faraday cup to protect the powder from the ion-beam before irradiation. Ar gas was injected into the ion gun, and the appropriate current density for treatment could be set by adjusting the discharge voltage and the ion-beam potential. After the ion gun reached a stable condition and the current density had reached a steady value, ion-beam irradiation was started while stirring the powder with a rotor blade. O_2 gas was injected from the bottom of the mixing bowl. After a predetermined period, Ar and O_2 gas injection was terminated. The irradiated HDPE powder was then premixed in a container with dried nylon 66 pellets at a predetermined weight ratio. Finally, the mixed powder was blended in a twin screw extruder (PRISM) at 280 °C.

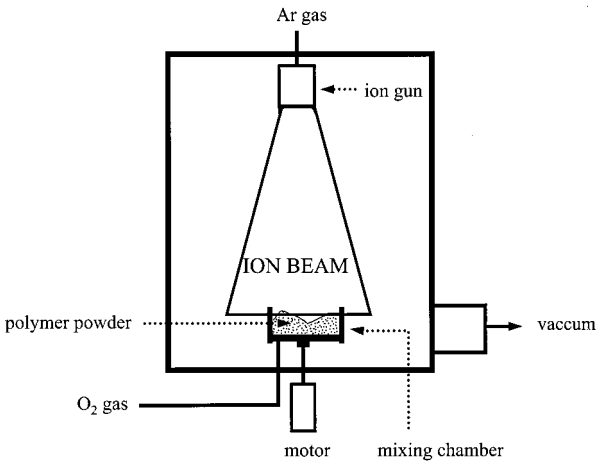

Figure 1. Schematic diagram of the ion-beam irradiation reactor.

Thermal Properties. Differential scanning calorimetry (DSC) studies of the thermal characteristics were performed using a DuPont 2910 DSC controlled with a 2100 thermal analyzer. The heating rate was 10 °C/min. Every thermogram was repeated at least twice to verify the reproducibility of the measurements. A DuPont 2950 thermal gravimetric analyzer was also used to observe the degradation of the samples. The heating rate was 10 °C/min, and the samples were heated to 600 °C.

Scanning Electron Microscopy. Scanning electron microscopy (SEM) observations of the composite samples were performed on a Hitachi S-2500 C model. The fractured surfaces of the blends were prepared by using cryogenic fracturing in liquid nitrogen followed by a coating with gold in an SPI sputter coater. The morphology was determined using an accelerating voltage of 15 keV.

Molecular Weight Distributions (MWD). Molecular weight distributions were determined by high-temperature gel permeation chromatography (GPC) using a differential refractive index detector. The system consisted of a Waters 150C ALC/GPC equipped with two Styragel columns (HT4 and HT5). The system was calibrated at 140 °C using some polystyrene standard materials (Polymer Laboratories). Samples were prepared by dissolution of 40 mg of polymer in 20 mL of a solvent, *o*-dichlorobenzene. The flow rate was 0.3 mL/min.

X-ray Photoelectron Spectroscopy (XPS) and Wide-Angle X-ray Scattering. The chemical components on the surface of the ion-beam-treated HDPE were analyzed by using XPS, and the spectra were recorded with a Surface Science 2803-S spectrometer ($h\nu = 1.5$ keV). A basic pressure of 2×10^{-10} Torr was maintained during the analysis, and the energy resolution was 0.48 eV. The XPS spectra were referenced to the main component of the C 1s peak of HDPE at a binding energy of 284.6 eV. The irradiation treatment generally resulted in a small shift of all the peaks (up to ca. 0.6 eV) toward higher binding energies, implying an increased conductivity for the modified surfaces. Overlapping peaks were

resolved by using a peak synthesis method based on Gaussian peaks.

Rheometry. The rheological properties were measured using a UDS200 (Physica, Germany) rheometer on which a 25 mm diameter cone and plate were mounted. The frequency range was set at 0.1−100 rad/s, and the applied strain was 5%. Before the measurement, the samples were prepared using a compression molder at 280 °C. The measurements were done under a nitrogen atmosphere.

Mechanical Properties. Testing of the mechanical properties of the blends was undertaken using an Instron Universal Testing Machine (model 4204) at a constant temperature. A crosshead speed of 10 mm/min was used. The tensile specimens were injection molded using a Mini-Max molder (CS-183). All the reported results are averages of at least seven measurements.

FT-IR spectrum. FT-IR spectra were obtained using a Bruker 200 spectrometer (IF 66) with an average of 200 scans at a resolution of 4 cm^{-1}. Attenuated total-reflection (ATR) adsorption spectra were recorded using an ATR accessory at a reflection angle of 30°.

Correlation between Rheology and Morphology. In polymer blends, most of the common polymers are incompatible, so they form multiphase systems. In the case of two components, the minor phase is usually dispersed in the form of spherical inclusions of different sizes into the major phase (matrix). Since the ultimate properties of the blends depend on the size distribution of the minor phase and the interfacial tension between components, good insight into the relationship between the blend morphology and its rheological behavior is essential to optimize the final physical properties of the blends. The relationship is reciprocal in the sense that the applied flow history can change the blend morphology while the two-phase structure affects, in turn, the rheology.[17] Recent advances in the field of polymer-blend rheology, based on the use of theoretical models, have allowed us to obtain quantitative relationships between linear rheological properties on one hand and interfacial properties on the other hand.[18] Thus, in principle, rheological data can be used to evaluate the average particle size and/or the interfacial tension; i.e., if a rheological model and information about the size of the dispersed phase are provided, the interfacial tension between the blend components can be determined.

The rheology of heterophase media is based on two different theoretical approaches. The first is based on the emulsion model (Oldroyd,[19] Choi and Schowalter,[20] Palierne[21]), and the second is based on a more generally applicable constitutive equation for blends with complex interfaces (Doi and Ohta,[22] Lee and Park[23]). In 1990, Palierne[21] published a model which has become the most widely used rheological model for polymer blends with a matrix and spherical inclusions. This model leads to an equation relating the linear viscoelastic material functions of the blend and its components to the interfacial properties and to the sphere-size distribution of the inclusions. This model has been successfully applied to describe the rheological behavior of polymer blends and to obtain the interfacial tensions or the dispersed particle sizes. Another model by Choi and Schowalter[20] deals with emulsions of two Newtonian fluids, but it predicts an elastic contribution, which is attributed to the form relaxation of the inclusions, in the rheological response. In this study, we obtain values for the interfacial tension in blends by using both the Palierne model and the Choi and Schowalter model, the latter being modified later by Gramespacher and Meissner[24] and by Gleinser et al.[25] Though another model by Lee and Park,[23] which is based on the Doi and Ohta model[22] which deals with an equal mixture of two immiscible fluids, is more versatile for describing various types of flows in immiscible blends, it has not been tried here because it has an empirical fitting parameter related to the shape relaxation of the deformed droplets. This is discussed in another report.[26]

The Palierne model[21] describes the complex modulus of molten blends, G_B^*, as a function of the complex modulus of each phase, G_M^* for the matrix, and G_D^* for the dispersed phase. The viscoelasticities of both phases, the hydrodynamics interactions, the droplet sizes and size distribution, and the interfacial tension are included in this formulation, but steric interactions and anisotropic effects which occur often in concentrated systems are not included. This limits the use of the Palierne model to moderate concentrations.[27−29] The interfacial tension, α, is the sole parameter describing the interfacial properties between the components.[29] If the effects of gravity and inertia are neglected, G_B^*can be expressed as a function of the volume fractions, ϕ_i , of droplets of radius R_i by[28]

$$G_B^*(\omega) = \frac{1 + 3\sum_i \phi_i H_i^*(\omega)}{1 - 2\sum_i \phi_i H_i^*(\omega)} G_M^*(\omega) \quad (1)$$

where H_i^* is given by

$$H_i^*(\omega) = \{4(\alpha/R_i)[2G_M^*(\omega) + 5G_{D^*}(\omega)] + [G_D^*(\omega) - G_M^*(\omega)][16G_M^*(\omega) + 19G_I^*(\omega)]\}/\{40(\alpha/R_i)[G_M^*(\omega) + G_D^*(\omega)] + [2G_D^*(\omega) + 3G_M^*(\omega)][16G_M^*(\omega) + 19G_I^*(\omega)]\} \quad (2)$$

with α being the interfacial tension between the two polymer blend components and $G^*(\omega)$ the complex shear modulus, $G^*(\omega) = G'(\omega) + iG''(\omega)$, at a given frequency ω. Since a small-amplitude, oscillatory flow does not affect the morphology, it can be used to study the effect of the morphology on the rheology in a nondestructive manner. Equation 1 can only be used for linear viscoelasticities, that is, for cases of small-amplitude, oscillatory shear flows.[27] Therefore, this model cannot predict the morphological changes during the flow. However, we are interested in the interfacial tension after blending and not in the morphology changes during the blending, so we can use the model.[28] The summation is carried out over the distribution of particle sizes (ϕ_i being the volume fraction of particles of radius R_i). For distributions which are not too broad (the polydispersity in size, d_v/d_n, where d_v is the volume-averaged diameter and d_n is the number-averaged diameter, does not exceed 2.3), the sum over (ϕ_i , R_i) in eq 1 can be replaced by a single term $H(\phi, R_v)$, where ϕ is the total volume fraction of inclusions and R_v is the volume-averaged particle radius.[27−29]

The emulsion model developed by Choi and Schowalter[20] is basically derived for two Newtonian liquids. However, the interfacial tension influences the viscoelastic properties only at low frequencies. In that frequency range, the loss modulus of a polymer melt is much larger than its storage modulus, which means that the viscoelastic behavior is predominantly governed by the zero-shear viscosity. Thus, the Choi−Schowalter model is applicable. Gramespacher and Meissner[24] took this into consideration to modify the loss modulus term of the Choi-Shcowalter model, and they expressed the complex modulus of the blend as

$$G_B^* = \phi G_D^* + (1 - \phi) G_M^* + G_{int}^* \quad (3)$$

where G_B^*, G_D^*, and G_M^* are the complex moduli of the blend and the individual components and G_{int}^* is the complex modulus of the contributions caused by the interfacial tension in the phase-separated blend. G_{int}^* is defined as follows:

$$G_{int}'(\omega) = \frac{\eta_b \omega^2 \tau_1 (1 - \tau_1/\tau_2)}{1 + \omega^2 {\tau_1}^2} \quad (4)$$

$$G_{int}''(\omega) = \frac{\eta_b \omega (1 - \tau_1/\tau_2)}{1 + \omega^2 {\tau_1}^2} \quad (5)$$

with

$$\eta_b = \eta_M[1 + \phi(5k + 2)/2(k + 1) + \phi^2 5(5k + 2)^2/8(k + 1)^2 - \phi^{8/3}21k(5k + 2)^2/4(k + 1)^2 + \phi^3 25(5k + 2)^3/32(k + 1)^3] \quad (6)$$

$$\tau_0 = \frac{\eta_M R}{\alpha} \frac{(19k + 16)(2k + 3)}{40(k + 1)} \quad (7)$$

$$\tau_1 = \tau_0\left(1 + \phi \frac{5(19k + 16)}{4(4k + 1)(2k + 3)}\right) \quad (8)$$

$$\tau_2 = \tau_0\left(1 + \phi \frac{3(19k + 16)}{4(4k + 1)(2k + 3)}\right) \quad (9)$$

This is the Choi−Schowalter model as modified by Gleinser et al.[25] We simply call it the CS model. Using this model, Gleinser et al. could obtain some correlations between the particle size and the trends in the interfacial tension for immiscible polymer blends of polystyrene and poly(styrene-*co*-acrylonitrile) with the compatibilizer (poly(styrene-*b*-methyl methacrylate)) included.

Results and Discussion

Surface Functionalization. A polymer surface irradiated with an ion beam depositing a high density of energy can be characterized as a highly reactive system in which the addition of a reactive gas induces many chemical reactions, thus introducing functional groups.[12,13] Normally, the functionalization is a heterogeneous reaction between a gas and a solid. A preliminary point to be discussed concerns the homogeneity within the XPS sampling depth of the modified samples. The penetration depth of an ion strongly relies on the class of the ion, the initial energy of the ion, and the material of the substrate to be treated. The estimated sampling depth for C 1s photoelectrons (for Al Kα photons at 1486.6 eV) is about 60 Å. It is slightly less for N 1s and O 1s photoelectrons.[30] We used the TRIM96 code[30] to calculate the penetration depth of low-energy 1 keV Ar^+ ions into HDPE. The maximum penetration depth calculated was 70 Å. Furthermore, there was no significant variation of the energy deposition along the track for a 1 keV Ar^+ ion; thus, the collisional term was the dominant one. These two facts convinced us that the modification of the irradiated layer was essentially homogeneous within the XPS sampling depth and that the thickness of the modified layer on the HDPE powder was quite thin.

The modified surface of the thin layer was suitably characterized by using XPS. Figure 2 shows the characteristic modification trend for the C 1s peaks from untreated and ion-beam-bombarded samples. The peak synthesis and the assignment of components were performed using the data in the literature.[8,10] The C 1s peak of the untreated HDPE was symmetric with a narrow full width at half-maximum, 1.54 eV. On the other hand, the C 1s peak of the ion-beam-irradiated HDPE (IBHDPE) powder was asymmetric because of carbon oxidation, and could be decomposed into one main peak and two small peaks by using a Gaussian peak-fitting code. The C 1s peak of the untreated sample is the C−C peak and was located at 284.6 eV. In the case of the irradiated HDPE powder, the binding energy of the carbon peak shifted slightly to higher energy (285 eV), and two other peaks appeared. The one at 286.5 eV was assigned as the C−O peak, and the other at 288.2 eV was assigned as the C═O peak. The energies of these new peaks in the treated sample indicate that the surface of the HDPE powder was sufficiently activated by Ar^+ ion irradiation to react with oxygen molecules, which produced covalent bonds between the carbon atoms and the oxygen atoms. This was also verified by the O 1s peak. Figure 2b shows the C═O peak at 532 eV and the C−O peak at 533.6 eV. The intensities of the C−C bond and the C−H bond decreased with irradiation while that of the carbon−oxygen bond increased. The variation of the O/C atomic ratio with the irradiation time is summarized in Table 1. The O/C atomic ratio increased with irradiation time, almost reached a plateau value and then slowly decreased. In the conventional ion-irradiation process, ion irradiation onto the polymer by reactive or inactive gases skews the C 1s peak at a binding energy of 284.6 eV to a higher energy between 285 and 289 eV and decreases its peak height, which means the main

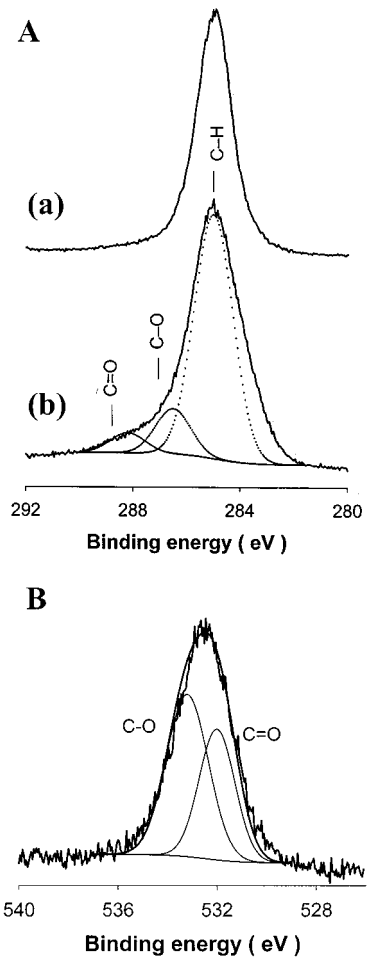

Figure 2. (A) XPS (C 1s) spectra of untreated HDPE (a) and of IBHDPE which had been ion-beam irradiated for 30 min (b). (B) XPS (O 1s) spectra of IBHDPE which had been ion-beam irradiated for 30 min.

Table 1. XPS Spectrum Results of Ion-Beam-Treated HDPE Powder

ion beam treatment time	atomic ratio (O/C)	content (%)[a]		
		C−H [b]	C−O	C═O
0 min	0.02	98		
10 min	0.09	88.86	9.37	1.77
20 min	0.12	84.26	12.48	3.27
30 min	0.17	82.49	12.06	5.44
2 h	0.20	80.65	13.42	5.93
4 h	0.13	83.85	11.63	4.51

[a] Realtive peak area in %. [b] Peak positions: C−H (285 eV), C−O (286.5 eV), and C═O (288.2 eV).

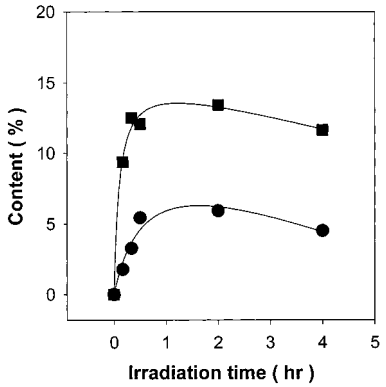

Figure 3. Variations in the concentrations of the C−O (■) and the C═O (●) functional groups at the surface of ion-beam irradiated powder (IBHDPE) with increasing irradiation time. The lines are guides for the eyes.

chemical bonds on the polymer surface have become carbon−carbon bonds.[8] The functional-group intensity variations with irradiation time are displayed in Figure 3. The amount of C−O bond in the irradiated HDPE is higher than that of C═O bond, and their ratio varies with irradiation time in the range between 2.2 and 5.3. It is certain that decrease in the functional groups concentration with long irradiation time is due to the fact that during irradiation, they disappear faster than they are being generated. This is attributed to degradation of the functional groups. The mechanism for this polymer degradation during ion-beam irradiation is different from the mechanism during thermal degradation. Gases composed of various compounds of carbon dioxide, methane, carbon monoxide, methyl formate, etc. have been reported to evolve from poly(methyl methacrylate) during ion-beam irradiation.[31] Gasification of the functional groups was also observed for HDPE surfaces.[32]

The functional groups formed on the surface of the HDPE powder by the ion-beam irradiation were also analyzed with FT-IR spectroscopy. Figure 4 shows the absorbance spectra for wavenumbers ranging from 1000 to 4000 cm^{-1}. The broad peak in the range from 3000 to 3500 cm^{-1} is ascribed to hydrogen bonding, which implies the existence of hydroxyl or carboxyl functional groups. To clarify the formation of new bonds due to ion implantation and chemical reactions, the differential spectra obtained by subtracting the absorbance spectra for pristine samples from those for treated specimens were investigated. The difference revealed that the ion-beam- irradiated HDPE surface had some new peaks at 1140, 1270, 1740, and 3400 cm^{-1}, which corresponded to C−O symmetric and antisymmetric stretching modes, the C═O stretching mode and the OH vibration mode, respectively. These peaks prove the surface functionalization of the HDPE powder.

Thermal Properties. DSC thermograms for both pristine and treated HDPE are shown in Figure 5. The melting temperature (T_m) did not change significantly, but the heat of melting (ΔH_m) decreased slightly with irradiation time (Table 2). This is ascribed to the crystallization being hindered by the functionalized molecules and to the difficulty in obtaining the proper conformation for crystallization because of the high molecular-weight molecules produced during the irradiation. Figure 6 shows the change in the molecular weight of HDPE with irradiation time as measured by GPC. As the irradiation time increased, the high molecular-weight portion increased slightly, indicating that a process of active site generation and active site recombination with other chain radicals occurred in the polymer chains during irradiation. In the case of γ-ray exposure, it was reported that the molecular weights decreased significantly with dose due to chain scission.[9,32] On the other hand, higher-energy ion-beam treatment induced severe chain cross-linking.[33] In comparison to other irradiation processes, low-energy ion-beam treatment does not induce a serious molecular-weight variation. The thermal stability of the irradiated HDPE powders is compared to that of pristine HDPE in Figure 7. Irradiated HDPE showed a slightly better

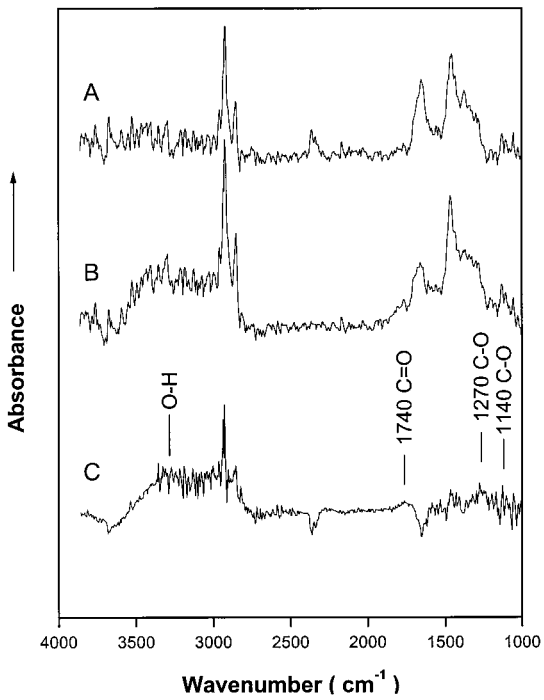

Figure 4. ATR FT-IR spectra of untreated HDPE (A) and IBHDPE which had been ion-beam irradiated for 30 min (B) and their corresponding difference spectrum (C).

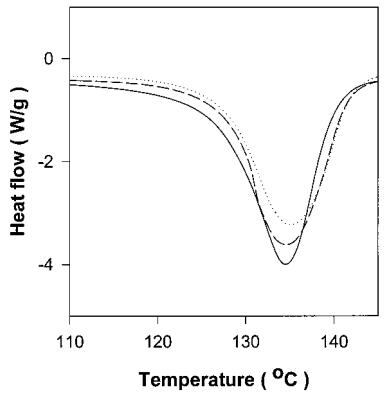

Figure 5. DSC endotherms of untreated HDPE (—), IBHDPE irradiated for 30 min (− −), and IBHDPE irradiated for 2 h (···).

Table 2. Changes in T_m and ΔH_m (J/g) of the Ion-Beam-Treated HDPE with Respect to Irradiation Time.

irradiation time	T_m (°C)	ΔH_m (J/g)
0 min	134.54	194.5
30 min	134.57	189.5
1 h	134.58	182.5
2 h	135.17	178.6

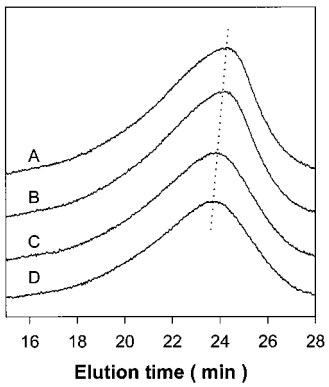

Figure 6. GPC curve of untreated HDPE (A), IBHDPE irradiated for 30 min (B), 2 h (C), and 4 h (D). The dotted line is a guide for peak maximum.

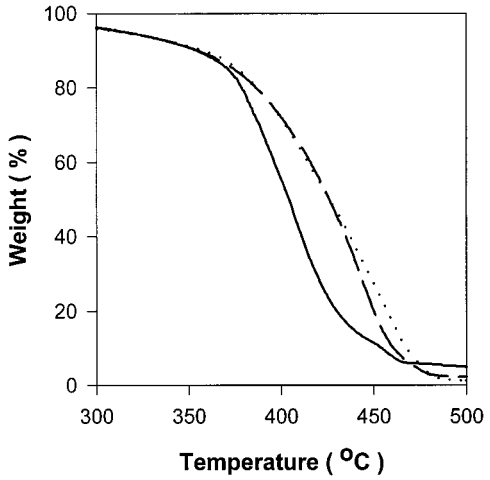

Figure 7. TGA thermograms of melt HDPE (—), and IBHDPE irradiated for 30 min (– –) and 2 h (···).

stability than untreated HDPE, which was also ascribable to the molecular-weight change.

Rheological Properties. The data for the dynamic viscosity of different blends at 280 °C are displayed in Figure 8. The pure polymers show almost constant dynamic viscosity at low shear rates, but shear thinning behavior at high shear rates. Ny66 is less shear thinning than HDPE. Ion-beam-treated HDPE (IBHDPE) shows almost the same behavior as untreated HDPE though the viscosity values are large, possibly due to the high molecular-weight portion produced during the irradiation. Comparison of the plateau viscosity with those of the pure components indicates that the mixtures show a positive deviation from the linear mixing rule. According to the emulsion model, the zero-shear viscosity of the mixture should be higher than those of the pure components. Although most polymer blends generally show a higher viscosity at low concentration and a positive deviation from the linear mixing rule, that is not always the case.[34] The viscosity–concentration dependence of immiscible polymer blends is not fully understood yet and merits further study.

A comparison of the dynamic viscosities of two groups (IBHDPE/Ny66 and untreated HDPE/Ny66 blends) produces some facts worthy of note. Most IBHDPE/Ny66 blends show higher viscosities than untreated HDPE/Ny66 blends, which is ascribable to different molecular-weight distributions, IBHDPE having the wider molecular weight distribution as mentioned before. However, the 50/50 wt % HDPE/Ny66 concentration blends show

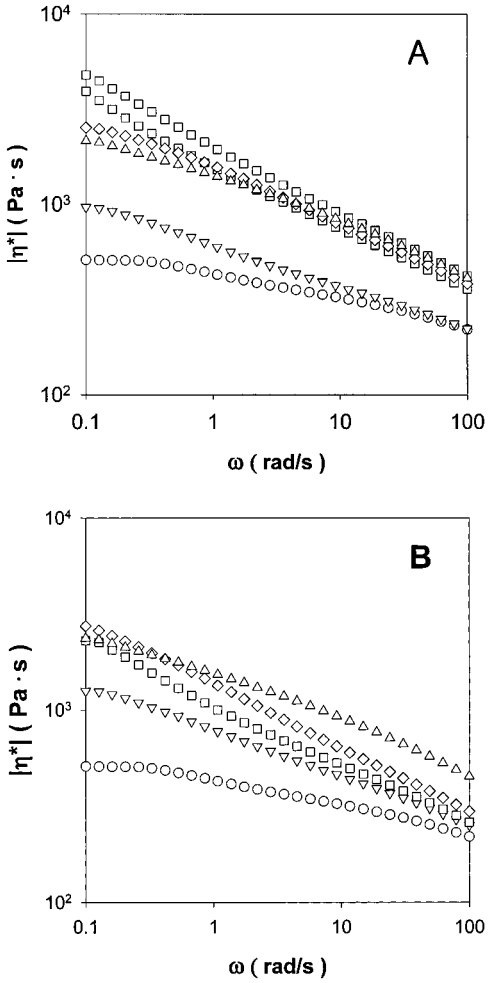

Figure 8. Dynamic viscosity ($|\eta^*|$) for different blends at 280 °C. (A) untreated HDPE/Ny66 blends: Ny66 (○), HDPE/Ny66 (20/80 wt %) (▽), HDPE/Ny66 (50/50 wt %) (□), HDPE/Ny66 (80/20 wt %) (◇), and HDPE (△). The two plots for the 50/50 wt % blend show the scattering of data at this composition. (B) IBHDPE (30-min irradiation)/Ny66 blends: Ny66 (○), IBHDPE/Ny66 (20/80 wt %) (▽), IBHDPE/Ny66 (50/50 wt %) (□), IBHDPE/Ny66 (80/20 wt %) (◇), and IBHDPE (△).

a striking difference between the treated and untreated blends. The data for the dynamic viscosity of IBHDPE blends were reproducible while those for untreated HDPE/Ny66 blends were scattered. Also, the maximum viscosity appeared at a 50/50 wt % ratio for untreated HDPE/Ny66 blend whereas it appeared at an 80/20 wt % ratio for the IBHDPE/Ny66 blend. Utracki stated that in immiscible polymer blends without interlayer slip, a maximum in the viscosity vs composition curve occurred at the phase inversion concentration.[34] The critical concentration for phase inversion can be calculated with some semiempirical equations.[34–36] Using Utracki's method, the critical concentration for the HDPE/Ny66 system is ca. 53 wt %, quite close to the experimental value. Around the phase inversion concentration, a region in which the phase behavior is complex, possibly co-continuous, is expected. Thus, the structure of the concentrated system is different in this region (50:50 wt % blend) for the untreated HDPE/Ny66 blend. In contrast, IBHDPE/Ny66 blends show progressive positive deviation of the viscosity from the linear mixing rule. The data were quite reproducible for IBHDPE/Ny66 blends, even for a 50/50 wt % ratio. We ascribe this to the compatibilizing action of IBHDPE which stabilizes the morphology, as will be shown later.

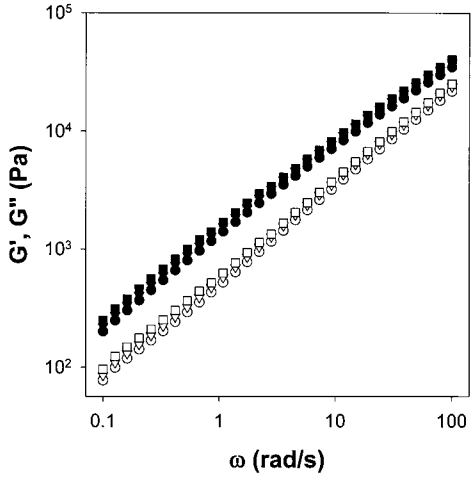

Figure 9. Storage modulus G' of untreated HDPE (○), IBHDPE (30-min irradiation) (▽), and IBHDPE (2 h irradiation) (□); loss modulus G'' of Ny66 (●), untreated HDPE (●), IBHDPE (30-min irradiation) (■), and IBHDPE (2-h irradiation) (■). Measurement temperature was 280 °C.

Instead of totally immiscible blends, IBHDPE forms more or less compatibilized blends featuring different rheological behaviors.

The frequency dependence of the dynamic moduli for untreated HDPE and IBHDPE are represented in Figure 9. The longer the ion-beam irradiation time, the higher the moduli of IBHDPE. This is in agreement with the molecular-weight change. Because of the wide MWD, the behavior of the dynamic modulus does not follow that of a typical homogeneous polymer melt. The frequency dependences of the dynamic moduli for the blends are shown in Figure 10. IBHDPE (30 min irradiation) and untreated PE melts show similar behaviors at low frequency. On the other hand, their blends show more relaxed behaviors at low frequency. For IBHDPE/Ny66 blends, the blend with an 80/20 wt % ratio has the largest values for the dynamic modulus at low frequencies. The peculiar thing for IBHDPE/Ny66 blends is that modulus values for the composition of a 50/50 wt % are smaller than those of an 80/20 wt % blend whereas the untreated HDPE/Ny66 blend at the 50/50 wt % composition shows the highest modulus values. This behavior is the same as that of the dynamic viscosity due to the unstable morphology around the critical concentration. Figure 11 gives plots of log G' vs log G'' for IBHDPE/Ny66 and untreated HDPE/Ny66 blends. In the low-frequency region, we observe that blends move away from the homopolymer plot, which

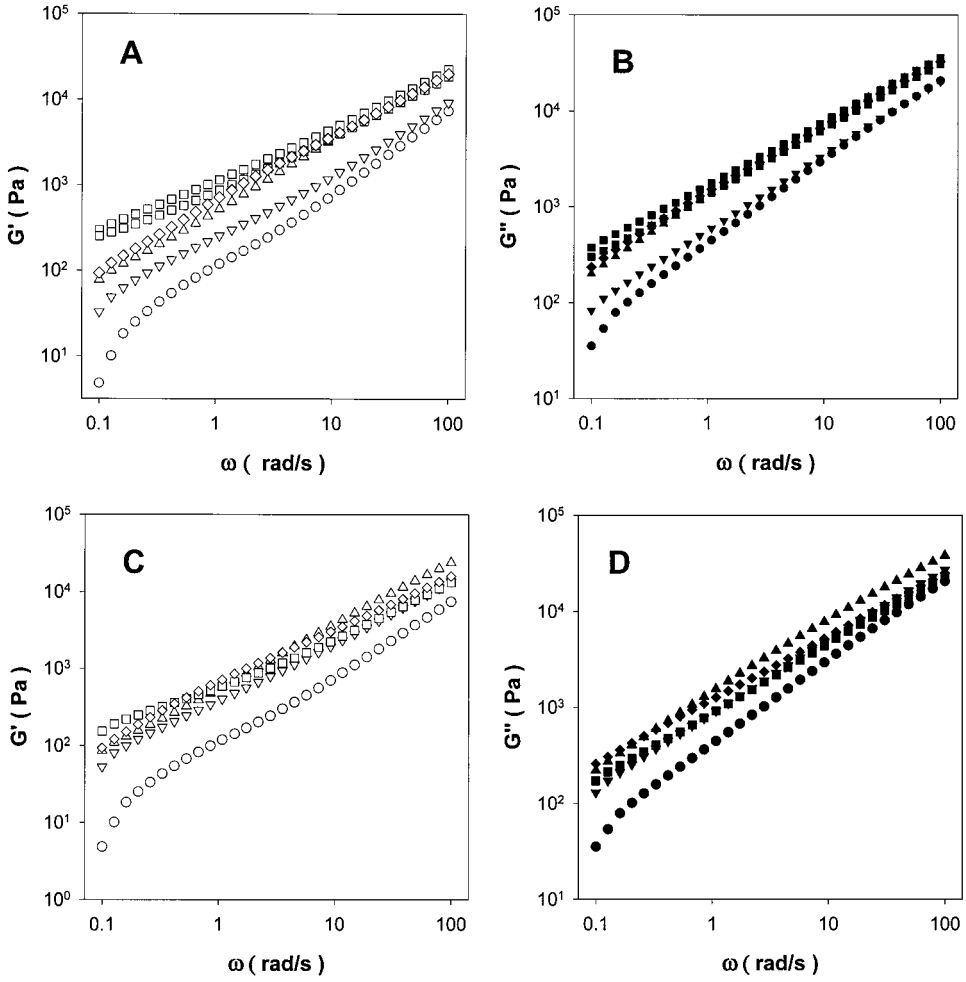

Figure 10. (A) Storage modulus G' of Ny66 (○), untreated HDPE (△), HDPE/Ny66 (20/80 wt %) blend (▽), HDPE/Ny66 (50/50 wt %) blend (□), and HDPE/Ny66 (80/20 wt %) blend (◊). The two plots for the 50/50 wt % blend show the scattering of data at this composition. (B) Loss modulus G'' of Ny66 (●), HDPE (▲), HDPE/Ny66 (20/80 wt %) blend (▼), HDPE/Ny66 (50/50 wt %) blend (■), and HDPE/Ny66 (80/20 wt %) blend (♦). The two plots for the 50/50 wt % blend show the scattering of data at this composition. (C) Storage modulus G' of Ny66 (○), IBHDPE (30-min irradiation) (△), IBHDPE/Ny66 (20/80 wt %) blend (▽), IBHDPE/Ny66 (50/50 wt %) blend (□), and IBHDPE/Ny66 (80/20 wt %) blend (◊). (D) Loss modulus G'' of Ny66 (●), IBHDPE (30-min irradiation) (▲), IBHDPE/Ny66 (20/80 wt %) blend (▼), IBHDPE/Ny66 (50/50 wt %) blend (■), and IBHDPE/Ny66 (80/20 wt %) blend (♦). Measurement temperature was 280 °C.

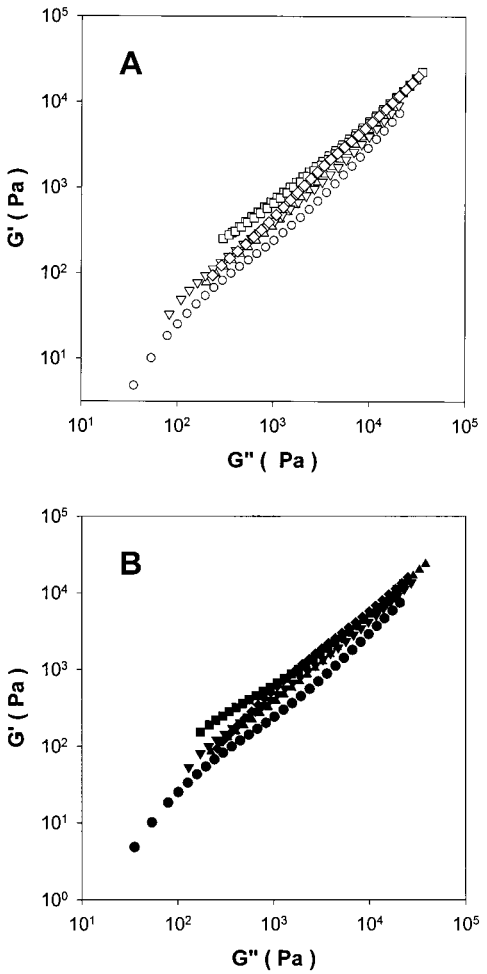

Figure 11. Log G' vs log G'': (A) Ny66 (○), untreated HDPE (△), HDPE/Ny66 (20/80 wt %) blend (▽), HDPE/Ny66 (50/50 wt %) blend (□), and HDPE/Ny66 (80/20 wt %) blend(◇); (B) Ny66 (●), IBHDPE (30-min irradiation) (▲), IBHDPE/Ny66 (20/80 wt %) blend (▼), IBHDPE/Ny66 (50/50 wt %) blend (■), and IBHDPE/Ny66 (80/20 wt %) blend (♦). Measurement temperature was 280 °C.

means a heterogeneous structure has developed.[37] In the low-frequency region, the blend with a 50/50 wt % ratio shows the greatest departure from the homopolymer plot. From these results, it is evident that the blends of IBHDPE/Ny66 have morphologies that are different from those of untreated HDPE/Ny66 blends.

Morphology and Interfacial Tension of the Blends. One of the most popular methods for making a compatible polymer blend is to provide some interaction between two immiscible polymers, which brings about a reduction in the total free energy.[16] There are the general ways to improve or induce the interaction. Polyethylene is a very hydrophobic, nonpolar material, and it is inherently immiscible with polar nylon 66. The addition of maleic anhydride groups to the polyolefin backbone has been widely used to provide some kind of interaction between polyolefins and polyamides.[38] This process is very important in commercial applications due to its unique combination of low cost, high activity, and good processability.[3,5] However, due to the inert nature of most polyolefins and poor control of the free-radical reaction, this maleic anhydride grafting reaction for functionalization causes many undesirable side reactions, such as β-scission, chain transfer, and coupling.[38] This kind of functional group grafting to HDPE is also quite complicated. In contrast, by using ion-beam assisted reactions, we can simply provide some functional groups in the backbone of HDPE. Since some of the functional groups are carboxyl groups as well as carbonyl groups, some kind of interaction between the functionalized HDPE and the polyamide (Ny 66) is expected.

In an effort to verify this interaction between HDPE and Ny66, we investigated the morphology of the blends. SEM micrographs of the fractured surfaces of binary blends are shown in Figure 12. A few facts are worthy of note. First, the continuous phase is the nylon 66 phase in blends for which the HDPE phase is less than 50 wt %. For the blend with 20 wt % HDPE, the untreated HDPE blend shows large discrete domains of HDPE dispersed in the nylon 66 matrix. In HDPE/Ny66 blends, the poor interfacial adhesion due to poor interaction and immiscibility is evident from the many round holes around the dispersed HDPE phase. Surface functionalization by ion-beam-assisted gas reaction has a significant effect on the blend morphology. The size of the dispersed HDPE phase is remarkably reduced (from 2.2 to 0.45 μm) and the HDPE phase is very finely dispersed. Even when the phases are reversed (Ny66 is dispersed in a HDPE matrix), interfacial adhesion looks quite good. Though not shown here because of space limits, all blends of ion-beam-treated HDPE showed similar morphologies regardless of the treatment time. The interdispersion and the better adhesion clearly demonstrate the existence of some interaction between the treated HDPE and the Ny 66. This can be interpreted as some HDPE molecules having functional groups in the backbone act as a compatibilizer or an emulsifier. The role of an emulsifier is to reduce the size of the dispersed phase solely by decreasing the interfacial tension whereas the role of a compatibilizer is to reside at the interface and form a kind of interphase which significantly improves the interfacial and the mechanical properties of the immiscible blends.[1,7] Since the emulsifying agent does not necessarily help the interfacial adhesion, any mechanical-property improvement originating from a uniform dispersion will be marginal. Significant improvements in the mechanical properties of immiscible blends cannot be achieved without strong interfacial adhesion between the matrix and the dispersed phase. Thus, a compatibilizer must be added to the system to improve the mechanical properties. This will be more evident in the mechanical-property measurements discussed later.

The difference in the morphologies is related to different interfacial tensions. Theoretical models allow us to obtain quantitative relationships between linear rheological properties on one hand and morphological/interfacial properties on the other hand. Hence, the rheological data can be used to evaluate the average particle size and/or the interfacial tension. If the particle size is provided, the interfacial tension can be determined by fitting the theoretical predictions to the experimental data. We examined the 20/80 wt % HDPE/Ny66 blends at 280 °C because mechanical properties of IBHDPE/Ny66 blend at this composition exhibited a positive deviation from the linear mixing rule as shown later. Application of the theoretical models with only one adjustable parameter, namely the ratio (α/R), produced the results in Figure 13. The models satisfactorily described the behavior of the blend over the entire frequency range. Since the dynamic loss modulus G' is not sensitive to droplet deformation, we discuss the

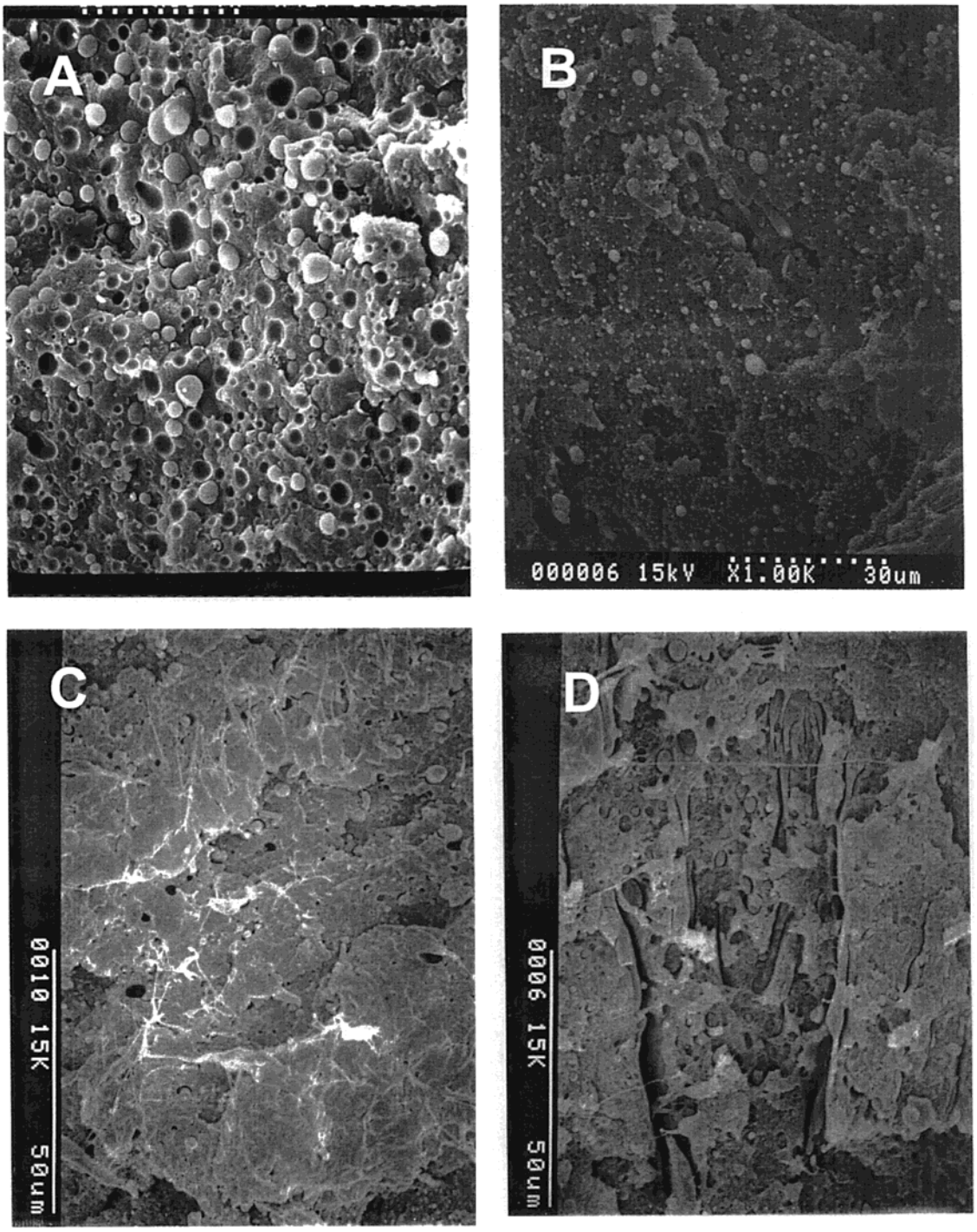

Figure 12. SEM micrographs of the fractured surfaces of binary blends: (A) untreated HDPE/Ny66 blend; (B) IBHDPE (30-min irradiation)/Ny66 (20/80 wt %); (C) IBHDPE/Ny66 (50/50 wt %); (D) IBHDPE/Ny66 (80/20 wt %).

storage modulus G' first. The appearance of a shoulder in G' at low frequency is directly related to the interfacial tension.[18] The enhancement of the elasticity at low frequencies, generally observed for multiphase systems, has been attributed to the deformability of dispersed particles.[26] At 280 °C, the volume-averaged droplet radius, R_v, is 2.21 μm for the untreated HDPE/Ny66 blend and 0.45 μm for the IBHDPE/Ny66 blend as mentioned above. In the model fitting, α/R was the optimized value. The optimized α values for the Palierne model were 4 mN/m for the untreated HDPE/Ny66 blend and 2.9 mN/m for the IBHDPE/Ny66 blend. These values are the same order as the value calculated for the untreated HDPE/Ny66 interfacial tension (6.4 mN/m at 280 °C) by using the harmonic-mean equation.[39] At low frequencies, the CS model shows better agreement with the experimental data than the Palierne model. However, the optimized interfacial-tension values were 2 mN/m for HDPE/Ny66 blend and 0.5 mN/m for the IBHDPE/Ny66 blend. The sensitivity of the model in estimating the value of the interfacial tension is related to the particle-size distribution. Using the volume-averaged particle size rather than the particle-size distribution was, however, proven to be less prone to error.[27] The model predictions are reasonable if the polydispersity of the particle-size distribution (volume-averaged particle size/number-averaged particle size) is less than 2.3.[27,28] In our case, it was less than 2 for both

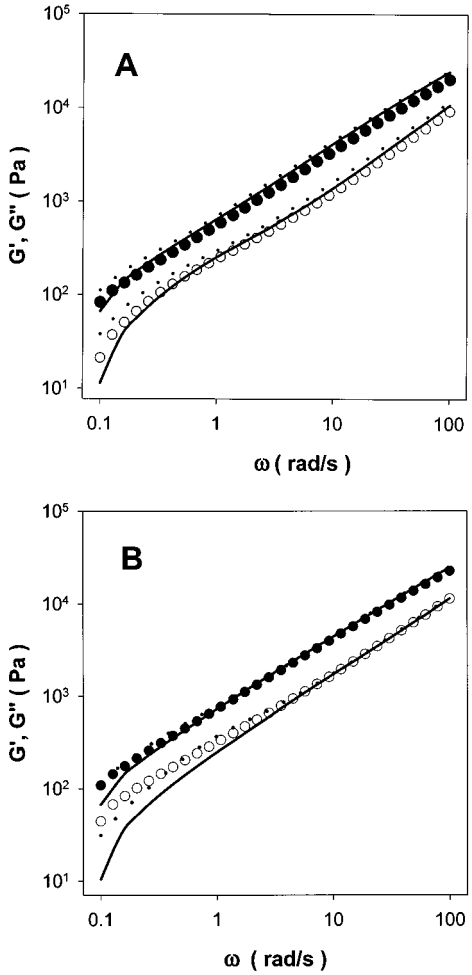

Figure 13. Comparison of model predictions with experimental data: (A) untreated HDPE/Ny66 (20/80 wt %) blend at 280 °C for the Palierne model (—) and the CS model (···); (B) IBHDPE (30-min irradiation)/Ny66 (20/80 wt %) blend at 280 °C for the Palierne model (—) and the CS model (···). Symbols are experimental data (G' (○) and G'' (●)).

cases, so we believe its effect to be small. Since the loss modulus of polymer melts is much larger than the storage modulus in the low-frequency range, the viscoelastic behavior at low frequency is predominantly governed by the zero-shear viscosity. The discrepancy between the predictions of the Palierne model and the experimental data is possibly due to the viscosity of the dispersed phase (HDPE) being higher than that of the matrix (Ny66). Because of the high viscosity of the dispersed phase, less deformation occurs. Thus, the CS model of the simple mixing rule plus the interfacial deformation matches the experimental data better than the Palierne model, which considers the deformation of the entire blend. However, the small interfacial tension values from the CS model require another explanation.[25] Both the Palierene model and the CS model implicitly assume that there is no coalescence between the dispersed droplets and that the droplets remain almost spherical, in another words, no interactions. The rheological properties of an emulsion strongly depend on the morphology. The behavior of an emulsion may also be affected by steric interactions or anisotropic effects which occur often in concentrated systems. In such cases, failures have been reported, thus limiting the use of the Palierne model to moderate concentrations.[29,40] Our experimental data show a similar discrepancy. At a concentration of 20 wt % HDPE, the terminal zone of the blend is shifted toward the low-frequency region, and the magnitude of the shoulder associated with the response of the interface is increased. At this concentration, the steric interaction cannot be excluded. This may explain the higher elastic modulus at low frequencies compared to Palierne model prediction. On the other hand, the contribution of the interface is negligible in the high-frequency region compared to those of the bulk properties of both phases (mixing rule).[25] Thus, there is no significant difference between the predictions of theoretical models and the experimental data. For the highly concentrated mixtures, another model by Lee and Park,[23] which takes into consideration the interactions between dispersed particles (coalescence and breakup), might be more suitable. This is under investigation and is to be reported in the future.[26] It should be emphasized, however, that these models corroborate the observation that the interfacial tension of the 20/80 wt % IBHDPE/Ny66 blend is less than that of the 20/80 wt % untreated HDPE/Ny66 blend. This proves the effect of ion-beam irradiation on HDPE.

Since the loss modulus is less sensitive to deformation, its variation with irradiation time is much less obvious than that of the storage modulus. Also, its variation with the blend composition is less remarkable. Both model predictions are in good agreement with the experimental data (Figure 13).

Mechanical Properties and Interfacial Interaction. The tensile strengths of the blends are shown in Figure 14a as functions of the composition. We observe a positive deviation from the rule of mixture, which is a sign of a typical compatible system. The tensile strength of ion-beam treated 20/80 wt % HDPE/Ny66 blend is remarkably higher than that of the pristine blend. Untreated HDPE blends show a negative deviation from the rule of mixture, which is a sign of an immiscible system. The tensile property of the blend containing 20 wt % IBHDPE is almost the same as that of virgin Ny66, which means a less expensive HDPE blend can perform as well as Ny66. Figure 14b shows the tensile strengths of the blends vs ion-beam irradiation time. They are almost constant. This is in accord with the fact that the functional group concentration soon reaches a plateau, as shown in Figure 3. Though the tensile modulus values for IBHDPE/Ny66 blends are increased (Figure 15b), they do not show a positive deviation from the linear mixing rule (Figure 15a). Thus, the improvement in the tensile strength of the blend is more or less ascribed to the improved interfacial adhesion between the two phases rather than to a reinforcing effect. This also affects the micromechanism for the formation of fractures in the blends. Blends can fail during monotonic loading as a result of a number of competing fracture micromechanisms, such as matrix cracking, dispersed-phase pullout, and breakage deformation.[27] Depending on the form in which the stored elastic strain energy in the dispersed HDPE phase is released and on the strength and the toughness of the dispersed-phase−matrix interface and the matrix itself, brittle fractures can result from the earliest fracture event and the distribution of flaws.[28] Figure 16 shows SEM micrographs of the fractured surface after tensile testing. For the immiscible untreated HDPE/Ny66 blend, the dispersed phase has a spherical shape. Evidently, the dispersed phase was not deformed at all while the matrix was deformed (Figure 16a,b). If the

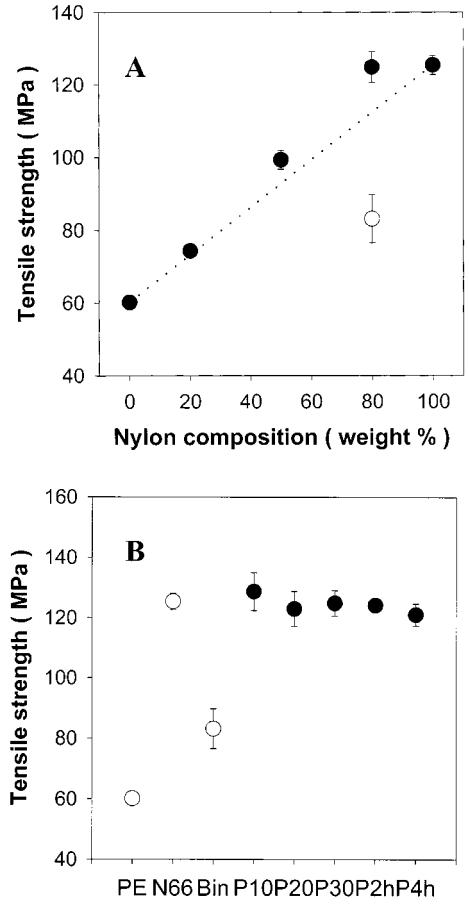

Figure 14. (A) Tensile strengths of the binary blends with different compositions. The empty symbol is for the untreated HDEP/Ny66 blend at the same composition. (B) Tensile strengths of 20/80 wt % IBHDPE/Ny66 blend with different irradiation time. Bin = Binary blend of untreated HDPE/Ny66, P10 = 10-min irradiated IBHDPE/Ny66 blend, P20 = 20-min irradiated IBHDPE/Ny66 blend, P30 = 30-min irradiated IBHDPE/Ny66 blend, P2h = 2-h irradiated IBHDPE/Ny66 blend, and P4h = 4-h irradiated IBHDPE/Ny66 blend.

force on the dispersed phase is sufficient to cause some debonding, breaking at the interface occurs. In contrast, for blends having good adhesion at the interface, the stress is transmitted to the dispersed HDPE phase and deforms it. In the case of IBHDPE/Ny66 blends, the dispersed phase (IBHDPE), as well as the matrix, is deformed. The break proceeded not only through the matrix but also through the dispersed phase. Hence, excess energy is consumed by plastic deformation of the dispersed HDPE phase. Figure 16 shows that most of the dispersed phase is deformed into elongated shapes. Pullout of the deformed dispersed phase requires extra energy to overcome the frictional force ascribed to the improved adhesion. As a result, the tensile strength of the system increases. Also, the elongation at break was larger for the IBHDPE blend because the deformed dispersed phase maintains contact with the sheath of the matrix surrounding it before breaking. In untreated HDPE blend systems, the propagating stress passes around the HDPE phase since the adhesion at the interface is quite poor. The HDPE phase does not maintain contact with the sheath of the matrix, and is easily pulled out. Thus, elongation does not increase. The simultaneous increases in the tensile strength (or tensile modulus) and the elongation are decisive evidence for improved adhesion due to the interaction at the interface.

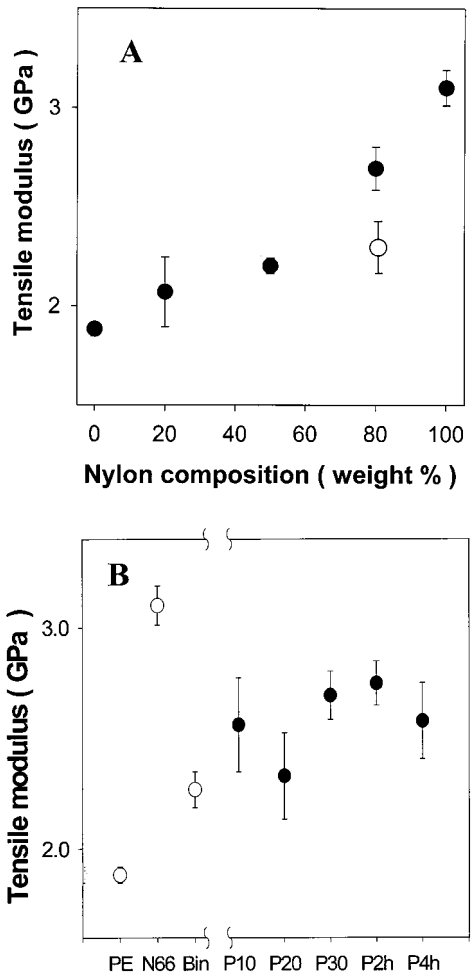

Figure 15. (A) Tensile modulus of the binary blends with different compositions. The empty symbol is for the untreated HDEP/Ny66 blend at the same composition. (B) Tensile modulus of 20/80 wt % IBHDPE/Ny66 blends with different irradiation time. Bin = Binary blend of HDPE/Ny66, P10 = 10-min irradiated IBHDPE/Ny66 blend, P20 = 20-min irradiated IBHDPE/Ny66 blend, P30 = 30-min irradiated IBHDPE/Ny66 blend, P2h = 2-h irradiated IBHDPE/Ny66 blend, and P4h = 4-h irradiated IBHDPE/Ny66 blend.

The enhancement of the mechanical properties and the fine dispersion of the HDPE phase in the blend of ion-beam-treated HDPE with Ny66 indicate that some interactions have occurred between the two phases. This enhancement can be described by two possible mechanisms: the occurrence of a reaction or an interaction such as hydrogen bonding. As verified by XPS and FT-IR results, the ion-beam-treated HDPE has oxygen-containing functional groups, C−O and CO−O, that can react or interact with polyamide functional groups (−CO−NH− or $-NH_2$). After the blend pellets were ground into fine powder and put in the Soxhlet extractor, the nylon 66 phase in the binary blend was extracted with boiling formic acid for a week. Figure 17 shows the FT-IR spectrum of the insoluble remnants. The peaks at 3300, 1650, and 1350 cm^{-1} are typical characteristic peaks of nylon 66. Those peaks were not observed in the spectrum from the remnants of the untreated HDPE/Ny66 blend. This implies that some other interactions stronger than hydrogen bonding exist between the two phases in the blend. We speculate that some chemical reactions, such as Scheme 1 may have taken place to form a kind of graft block copolymer acting at the interface as a compatibilizer, thus increas-

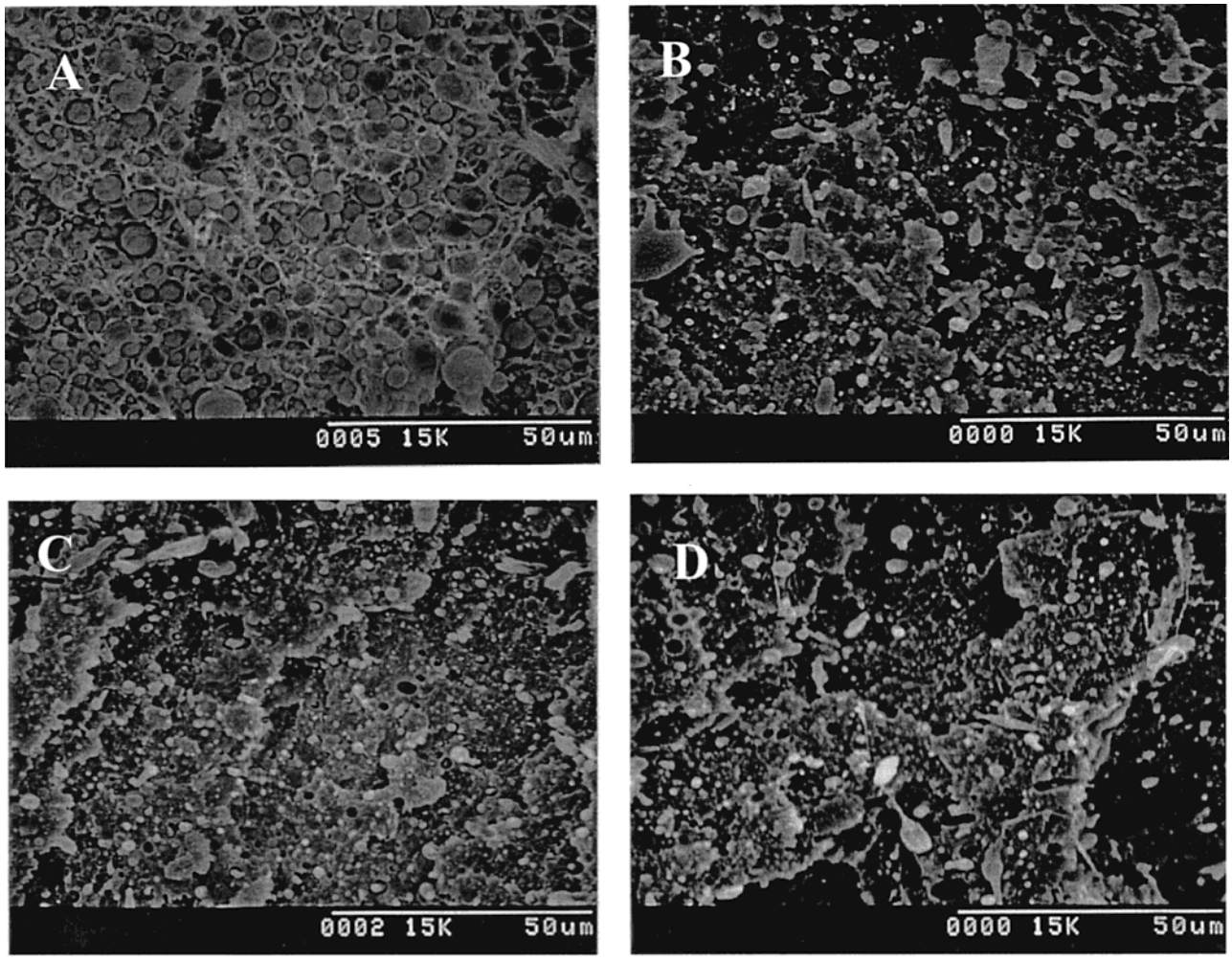

Figure 16. SEM micrographs of the fractured surfaces after tensile test: (A) untreated HDPE/Ny66 blend; (B) 10-min irradiated IBHDPE/Ny66 blend; (C) 30-min irradiated IBHDPE/Ny66 blend; (D) 2 h irradiated IBHDPE/Ny66 blend. The weight ratios of HDPE/Ny66 blends are all the same, 20/80 wt %.

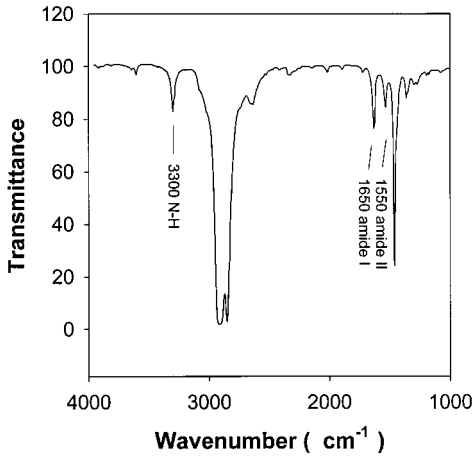

Figure 17. FT-IR spectrum of insoluble remnant of IBHDPE/Ny66 blend after Soxhlet extraction.

ing the interfacial adhesion and the mechanical properties of the blends.

Conclusions

In this study, we experimentally demonstrated that the ion-beam-assisted gas reaction technique caused surface modification of dispersed particles and remarkably changed the physical properties of immiscible

Scheme 1

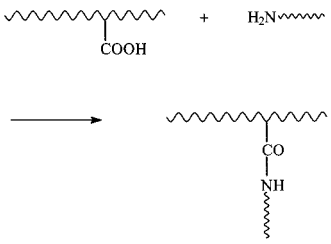

HDPE/Ny66 polymer blends by providing compatibility between the two phases. This newly discovered interaction is ascribed to surface functional groups containing carboxyl and carbonyl groups. Ion-beam-assisted gas reaction is a very efficient technique for changing polymer surface properties by incorporating functional groups. This simple modification route is characterized as a heterogeneous, solvent-free, and environmentally favorable process. Since the modification proceeds at a relatively shallow depth below the surface, the physical properties of the ion-beam-treated HDPE do not change remarkably. The interfacial properties of the HDPE/Ny66 blends are, however, significantly changed due to the strong adhesion at the interface and the reduced interfacial tension.

The interfacial tension was evaluated using emulsion models (Palierne model and CS model). Though the concentration was relatively high, both model predict

the linear viscoelastic data of HDPE/Ny66 blends pretty well. The values of the interfacial tension from the Palierne model were the same order as those calculated using the harmonic-mean equation. The values of the interfacial tension calculated for the IBHDPE/Ny66 blends were less than those calculated for untreated HDPE/Ny66 blends, which showed the effect of functionalization on the HDPE surface caused by ion-beam-assisted gas reaction.

Good adhesion at the interface enables the stress to be transmitted to the dispersed HDPE phase, and to deform it. Hence, extra energy is consumed by plastic deformation of the HDPE. Also, extra energy is consumed in the tensile extension process to overcome the larger frictional force due to better adhesion. As a result, the tensile strength of the system increases. Though not reported here, the impact property is also significantly increased.

On the basis of the FT-IR spectra of the Soxhlet extracted remnants, we believe that some chemical reaction may have taken place to form a kind of graft copolymer which acted at the interface to reduce the interfacial tension and to provide good adhesion. We conclude by noting a particularly useful aspect of the ion-beam-assisted gas-reaction route to polymer surface modification. It is quite unique and is a very efficient way to change the polymer surface properties. It can be used not only in polymer blend applications but also in other high performance polymer applications (adhesion, wear resistance, hydrophilicity, etc.). This merits further study.

Acknowledgment. This work was partly supported by KIST (No. 2E16520) and MOST (No. 2N20880). We acknowledge the helpful discussions with and comments by Professor Hyoung-Jin Choi at Inha University and Professor Junhan Jo at Dankook University.

References and Notes

(1) Paul, D. R., Bucknall, C. B., Eds. *Polymer Blends*; John Wiley & Sons: New York, 2000; Vols. I and II.
(2) Shonaike, G. O., Simon, G. P., Eds. *Polymer Blends and Alloys*; Marcel Dekker Inc.: New York, 1999.
(3) Utracki, L. A. *Commercial Polymer Blends*; Chapman & Hall: London, 1998.
(4) Araki, T.; Tran-Cong, Q.; Shibayama, M. *Structure and Properties of Multiphase Polymeric Materials*; Marcel Dekker Inc.: New York, 1998.
(5) Datta, S.; Lohse, D. J. *Polymeric Compatibilizers*; Hanser: Munich, Germany, 1996.
(6) Xanthos, M., Ed. *Reactive Extrusion*; Hanser: Munich, Germany, 1992.
(7) Utracki, L. A. *Polymer Alloys and Blends*; Hanser: New York, 1989.
(8) Bertoti, I.; Menyhard, M.; Toth, A. In *Handbook of Surface and Interface Analysis*; Riviere, J. C., Mihra, S., Eds.; Marcel Dekker: New York, 1998, Chapter 8.
(9) Valenza, A.; Spadaro, G.; Calderaro, E.; Acierno, D. *Polym. Eng. Sci.* **1993**, *33*, 845; Spadaro, G.; Acierno, D.; Dispenze, C.; Calderaro, E.; Valenza, A. *Radiat. Phys. Chem.* **1996**, *48*, 207.
(10) Young, R. P.; Slemp, W. S., In *Irradiation of Polymeric Materials*; Reichmanis, E., Frank, C. W., O'Donnell, J. H., Eds.; ACS Symposium Series 527; American Chemical Society: Washington, DC, 1993; pp 278−304.
(11) Lee, E. H.; Rao, G. R.; Hanser, L. K. *Trends Polym. Sci.* **1996**, *4* (7), 229.
(12) Koh, S. K.; Song, S.; Choi, W.; Jung, H. *J. Mater. Res.* **1995**, *10*, 2390.
(13) Koh, S. K.; Park, S.; Kim, S.; Choi, W.; Jung, H., Pae, K. *J. Appl. Polym. Sci.* **1997**, 64, 1913.
(14) Choi, W.; Koh, S.; Jung, H. *J. Vac. Sci. Technol.* **1996**, *A14* (4), 2366.
(15) Park, S.; Koh, S.; Pae, K. *Polym. Eng. Sci.*, **1998**, 38, 1185.
(16) Coleman, M. M.; Graf, J. F.; Painter, P. C. *Specific Interactions and the Miscibility of Polymer Blends*; Technomic: Lancaster, PA, 1991.
(17) Wilkinson, A. N.; Ryan. A. J. *Polymer Processing and Structure Development*; Kluwer Academic Publishers: Dordrecht, The Netherlands, 1998.
(18) Carreau, P.J.; DeKee, D.C. R.; Chbara, R.P. *Rheology of Polymeric Systems*; Hanser:Munich, 1997.
(19) Oldroyd, J. C. *Proc. R. Soc. London* **1953**, *A218*, 122; **1955**, *A232*, 567.
(20) Choi, S. J.; Schowalter, W. R. *Phys. Fluids* **1975**, 18, 420.
(21) Palierne, J. F. *Rheol. Acta* **1990**, *29*, 204.
(22) Doi, M.; Ohta, T. *J. Chem. Phys.* **1991**, *95*, 1242.
(23) Lee, H. M.; Park, O. O. *J. Rheol.* **1994**, *38*, 1405.
(24) Gramespacher, H.; Meissner, J. *J. Rheol.* **1992**, *36*, 1127.
(25) Gleinser, W.; Braun, H.; Friedrich, C.; Cantow, H. J. *Polymer* **1994**, *35*, 128.
(26) Seo, Y.; Kim, H. J. To be submitted to *J. Rheol.*
(27) Graebling, D.; Muller, R.; Palierne, J. F. *Macromolecules* **1993**, 26, 320.
(28) Bousmina, M.; Bataille, P.; Supieha, S.; Schreiber, H. P. *J. Rheol.* **1995**, *39*, 499.
(29) Lacroix, C.; Aressy, M.; Carreau, P. J. *Rheol. Acta* **1997**, 36, 416.
(30) Ziegler, J. F.; Biersack, J. P.; Littmak, U. *The Stopping and Range of Ions in Solids*; Pergammon Press: New York, 1985.
(31) Fragala, M. E.; Compagnini, G.; Licciardello, A.; Puglisai, O. *J. Polym. Sci., Polym. Phys. Ed.* **1998**, *36*, 655.
(32) Hill, D. J. T.; Milne, K. A.; O'Donnell, J. H.; Pomery, P. J. In *Irradiation of Polymers*; Clough, R. L., Chalaby, S. W., Eds.; ACS Symposium Series 620; American Chemical Society: Washington DC, 1996; pp 130−138.
(33) Lee, E. H.; Rao, G. R.; Lewis, M. B.; Mansur, L. K. *J. Mater. Res.* **1994**, 9, 1043.
(34) Utracki, L. A. *J. Rheol.* **1991**, *35*, 1615.
(35) Paul, D. R.; Barlow, J. W. *J. Macromol. Sci.—Rev. Makromol. Chem.* **1980**, *C18*, 109.
(36) Metelkin, V. I.; Blekht, V. S. *Kolloid Zh.* **1984**, *46*, 476.
(37) Kim, J. K.; Lee, H. H.; Son, H. W.; Hand, C. D. *Macromolecules*, **1998**, *31*, 8566.
(38) Seo, Y.; Hwang, S. S.; Kim, K. U.; Lee, J.; Hong, S. *Polymer* **1993**, *34*, 1667.
(39) Wu, S. *Polymer Interface and Adhesion*; Marcel Dekker: New York, 1982.
(40) Bousmina, M.; Muller, R. *Rheol. Acta* **1996**, *35*, 369.

MA0013760